Structural and Compositional Changes during Hydrogenation/Dehydrogenation of the Li−Mg−N−H System

Jianjiang Hu, Yongfeng Liu, Guotao Wu, Zhitao Xiong, and Ping Chen*

Departments of Chemistry and Physics, National University of Singapore, Singapore 117542

Received: July 23, 2007; In Final Form: September 20, 2007

Structural and compositional changes in the Li−Mg−N−H system have been studied by probing the pressure composition isotherms at different hydrogenation/dehydrogenation stages. The results of X-ray diffractometry and Fourier transform infrared spectroscopy show that $LiNH_2$ and a ternary imide with the composition $Li_2Mg_2(NH)_3$ are reversibly formed and consumed in the hydrogen absorption/desorption processes. Chemical reactions have been proposed for hydrogen absorption and desorption, accordingly. The formation of solid solutions in the system is assumed based on structure and phase analysis.

Introduction

Hydrogen as an environmentally benign fuel has attracted tremendous efforts around the world for the development and implementation of advanced technologies to produce, store, and convert it. Nevertheless, the storage of hydrogen gas in a safe and efficient way proves to be a bottleneck in the on-board hydrogen supply.[1] As compared to physical approaches such as compression and liquefaction, solid-state hydrogen storage may have merits in terms of high volumetric and gravimetric hydrogen density.[2] Metal nitrides and imides with a strong hydrogen affinity add a group of chemicals to the family of solid-state hydrogen storage materials.[3] The $LiNH_2$−LiH system can reversibly deliver and absorb 6.5 wt % hydrogen, although the corresponding operation temperature is relatively high.[4] Substituting lithium amide by magnesium amide changes the thermodynamics of the dehydrogenation, which brought a step forward toward practical applications.[5−7] As demonstrated by different researchers, the enthalpy of hydrogen desorption decreases from 66 kJ/mol of H_2 for $LiNH_2$−2LiH to ca. 44 kJ/mol of H_2 for $Mg(NH_2)_2$−2LiH. The thermodynamic parameters predict that the dehydrogenation temperature of $Mg(NH_2)_2$−2LiH at 1 bar equilibrium H_2 pressure is ca. 90 °C, close to the operation temperature of proton exchange membrane (PEM) fuel cells.[8] This is one of the most promising hydrogen storage systems amid metal amide−hydride combinations. However, the stepwise dehydrogenation and slow kinetics need to be modified and overcome. Mechanistic investigation will certainly enhance the understanding of the corresponding reaction system and provide information for materials optimization.

In this study, we used an automatic Sieverts' apparatus for measurements of pressure− composition isotherms (PCI) of the $Mg(NH_2)_2$−2LiH system. By sampling at typical stages of hydrogenation and dehydrogenation, the chemical species at the respective stages were identified, which enable us to illustrate chemical events during hydrogen release and absorption.

Experimental Procedures

Materials. LiH was obtained from Sigma-Aldrich with 95% purity. $Mg(NH_2)_2$ was synthesized in-house by reacting magnesium powder (Sigma-Aldrich, 99%) with NH_3 (Union Carbon, 99%) at 300 °C. $Li_2MgN_2H_2$ was prepared by ball milling $Mg(NH_2)_2$ with LiH at a 1:2 molar ratio on a Retsch PM400 ball mill for 36 h, followed by dehydrogenation at 260 °C under vacuum in a homemade reactor.

Methods. The PCIs were obtained on a commercial Sieverts' automatic gas reaction system from Advanced-Materials Corp. FTIR measurements were conducted on a PerkinElmer FTIR-3000 unit in DRIFT mode (diffuse reflectance infrared Fourier transform). The powdery samples were loaded into the DRIFT in situ cell in a glovebox filled with Ar as a protective atmosphere and measured at a resolution of 4 cm^{-1}. For the X-ray diffraction measurements (Bruker D8 Avance X-ray diffractometer with Cu Kα radiation), about 50−70 mg of sample was pressed into pellets and fixed to the XRD sample holder. Thermogravimetric measurements were carried out on a TG-DTA/DSC LabSys (Setaram) at a heating rate of 5 °C/min. The sample loading was performed in a glovebox.

Hydrogenation and dehydrogenation were carried out on the Sieverts' automatic gas reaction system at 205 °C. The PCI experiments were stopped at certain points of hydrogen absorption/desorption, and samples were collected for further analysis. The sample loading for the PCI measurement was about 400 mg.

Results and Discussion

Characterization of $Li_2Mg_2(NH)_3$. It was reported in 1962 by Juza and Eberius that the ternary nitride LiMgN could react with NH_3 at 320−400 °C, resulting in a ternary imide with a composition of $Li_2Mg_2(NH)_3$.[9] The crystal parameters of $Li_2Mg_2(NH)_3$ were determined to be $a = 5.15$ Å and $c = 9.67$ Å. In our previous study on the compositional changes of the $Mg(NH_2)_2$−LiH system, an XRD pattern was obtained after reacting $Mg(NH_2)_2$ with LiH at a 1:1 molar ratio at ca. 330 °C.[10] Calculations based on the XRD results led to a tetragonal crystal structure with $a = 5.13$ Å and $c = 9.63$ Å, which is close to Juza and Eberius' results.

As will be discussed next, an intermediate having a similar structure to the solid residue of post-reacted $Mg(NH_2)_2$−LiH (1:1 molar ratio) was frequently observed in hydrogen absorption/desorption of the $Mg(NH_2)_2$−2LiH system. It is important to further elucidate the structure and composition of the phase

* Corresponding author. Tel.: +65 65165100; fax: +65 67776126; e-mail: phychenp@nus.edu.sg.

10.1021/jp075757s CCC: $37.00
Published on Web 11/16/2007

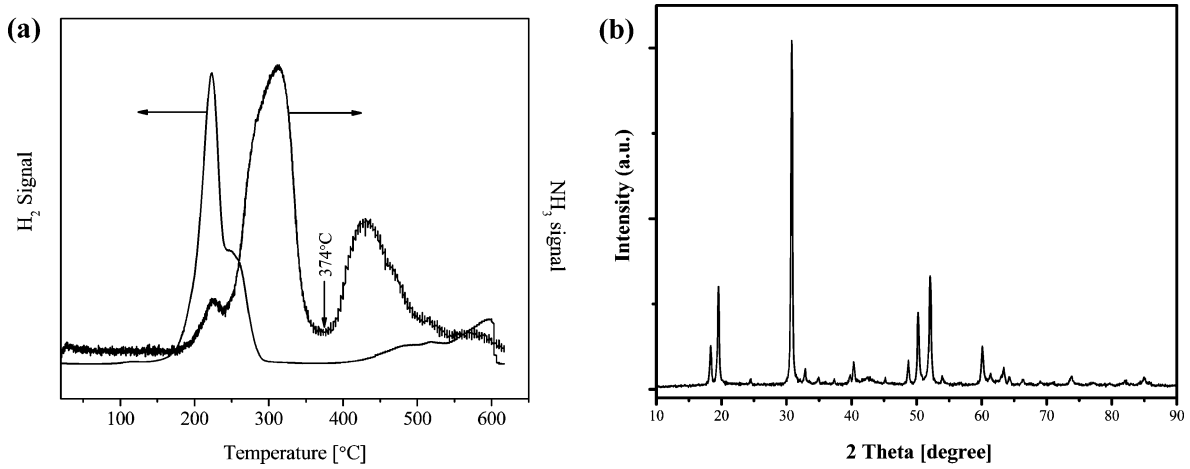

Figure 1. (a) TPD-MS measurement of the ball milled mixture of $Mg(NH_2)_2$-LiH at 1:1 molar ratio and (b) XRD pattern of the post-TPD (to 374 °C) sample.

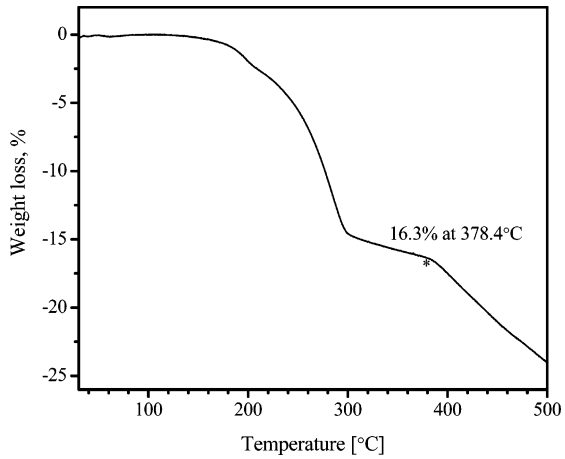

Figure 2. TG trace of the ball milled mixture of $Mg(NH_2)_2$-LiH at 1:1 molar ratio.

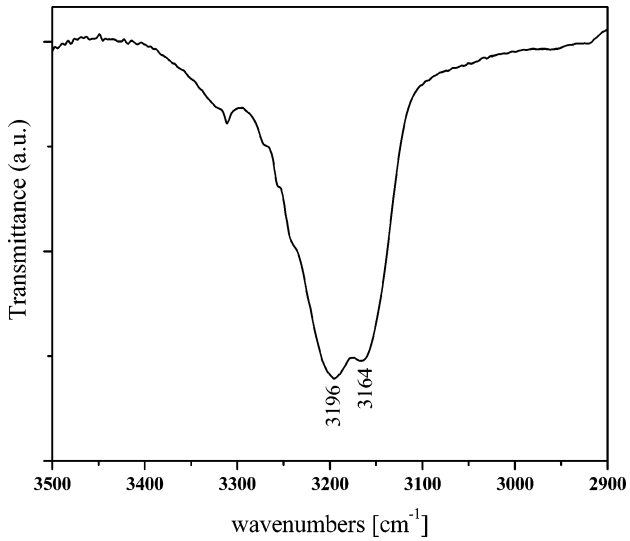

Figure 3. FTIR spectrum of the ball milled mixture of $Mg(NH_2)_2$-LiH at 1:1 molar ratio after TPD-MS test to 374 °C.

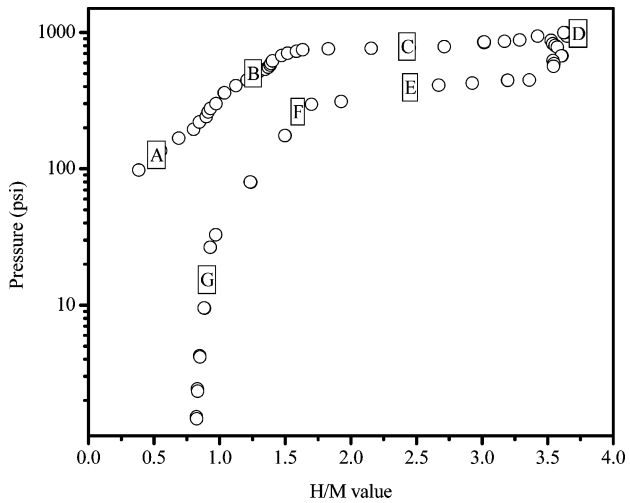

Figure 4. PCI curves of the Li−Mg−N−H system.

to better understand the chemical events in the Li−Mg−N−H system. In this context, a mixture of $Mg(NH_2)_2$ with LiH at a 1:1 molar ratio was ball milled for 12 h and subjected to a temperature programmed reaction. As shown in Figure 1a, hydrogen was released accompanied by the generation of NH_3. The NH_3 generation consists of two steps (i.e., before and after 374 °C). The XRD pattern of the sample collected at 374 °C (Figure 1b) exhibits a single-phase structure having the same peak positions as in ref 10. To determine the chemical composition of the new structure, a thermogravimetric measurement of the ball milled sample was conducted as shown in Figure 2. At 374 °C, just before the commencement of another step of thermal decomposition, the amount of weight loss was 16.3%. Combining the previous observations, the total chemical changes of the ball milled mixture may be described as follows:

$$2LiH + 2Mg(NH_2)_2 \xrightarrow{374\ ^\circ C} Li_2Mg_2(NH)_3 + NH_3 + 2H_2 \quad (1)$$

with a theoretical weight loss of 16.4% due to gas evolution, in agreement with thermogravimetric results. Figure 3 shows the FTIR spectrum of the ternary imide. Broad absorbances appear at 3164 and 3195 cm^{-1}, showing a typical N−H vibration.

Changes in Composition and Structure during the Hydrogen Sorption Process. The typical PCI curve of the Li−Mg−N−H system was reported previously.[6,11] There are two characteristic regions in the curve (i.e., a sloping region with H content from 0 to about 1.5 H atoms per $Li_2MgN_2H_2$ and a plateau with H content from 1.5 to 4.0 H atoms per $Li_2MgN_2H_2$). Shown in Figure 4 is the typical PCI curve of the Li−Mg−N system at 220 °C. Samples were collected at different intervals of hydrogenation (A−D) and dehydrogenation (E−G).

Different crystal structures of the ternary imide $Li_2MgN_2H_2$ can be obtained from the mixture of $Mg(NH_2)_2$−2LiH, depend-

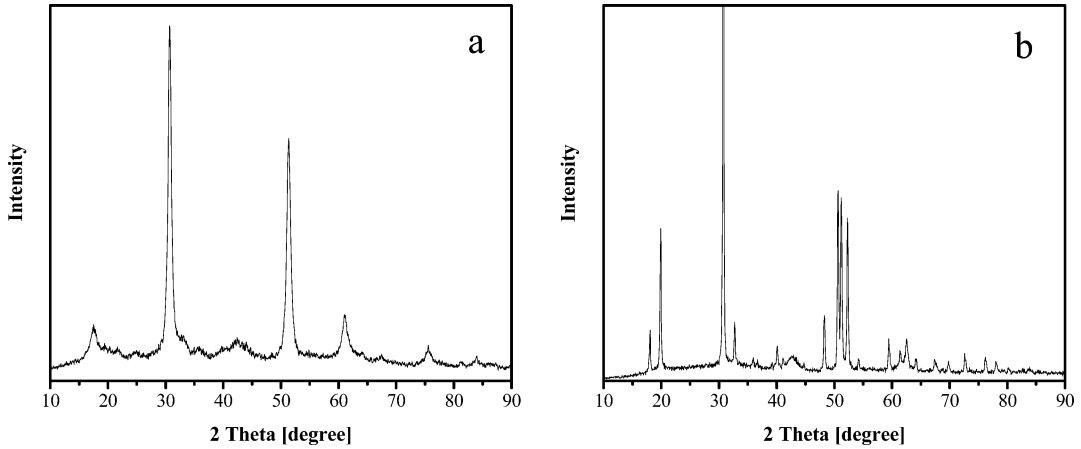

Figure 5. XRD patterns obtained from different preparation methods: (a) cubic structure and (b) orthorhombic structure.

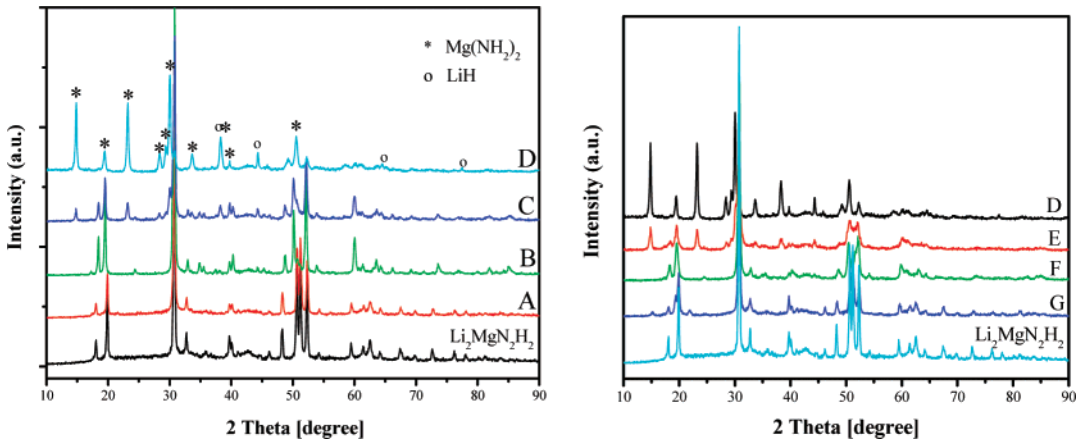

Figure 6. XRD patterns at different PCI stages (capital letters denote the sampling points of the PCI experiments).

ing on the preparation method.[12] In our first paper concerning the $Mg(NH_2)_2-2LiH$ system,[6] we reported a cubic structure with a lattice constant of 10.0398 Å (Figure 5a). The sample was obtained on the TPD apparatus, in which the mixture of $Mg(NH_2)_2$ and LiH was dehydrogenated dynamically by purging with Ar gas in a temperature ramp. Leng et al.[7] and Janot et al.[13] also observed this crystal structure separately. Another XRD profile with an orthorhombic structure (Figure 5b) was obtained from a sample collected under isothermal conditions (i.e., the mixture of $Mg(NH_2)_2-2LiH$ underwent dehydrogenation in a Sieverts' automatic gas reaction system). This structure was reported by Luo and Sickafoose,[11] Rijssenbeek et al.,[12] and Aoki et al.[14] In this study, we used the ternary imide with an orthorhombic structure as the starting material for PCI experiments. XRD measurements were conducted to study the phase changes at different hydrogen sorption stages.

As shown in Figure 6, the pattern of the sample collected at point A ($H = 0.33$) remains almost unchanged from the starting imide. At point B ($H = 1.35$), the pattern resembles that of the imide at first glance. However, a close examination of the two patterns reveals that they are different from each other, most prominently at about 20 and 50° 2θ. In fact, the XRD pattern at point B represents the crystal structure of another ternary imide with the composition of $Li_2Mg_2(NH)_3$ described in the prior section. The imide $Li_2Mg_2(NH)_3$ phase persisted in the sample of the next stage of hydrogenation at point C ($H = 2.60$) along with the emergence of magnesium amide and lithium hydride. It disappeared when hydrogenation was completed at point D ($H = 3.90$). Magnesium amide and lithium hydride are the only phases detected by XRD at point D. For the dehydrogenation process, the XRD patterns show the reverse phase changes from the amide and the hydride (at points D and E, $H = 3.90$ and 2.65, respectively) via $Li_2Mg_2(NH)_3$ (at points E−G, $H = 2.65$, 1.5, and 0.86, respectively) to $Li_2MgN_2H_2$, demonstrating the reversible phase changes in the system. It is interesting that both imides $Li_2MgN_2H_2$ and $Li_2Mg_2(NH)_3$ coexist in the XRD pattern at $H = 0.86$ (point G). In addition, it can be seen from Figure 6 that the intensity of the characteristic diffraction peaks of the LiH phase at 38.0 and 44.2° increase during the hydrogenation step (A → B → C → D) and decrease in the dehydrogenation step (D → E → F → G), indicating the formation and consumption of LiH. While the major diffraction peaks of LiH at 38.0 and 44.2° are discernible for samples B and F, it is difficult to see for sample G, which is due to the low concentration at the stage close to full dehydrogenation.

The vibrations of N−H bonding in the metal amides and imides are infrared active and can therefore be referred to for the identification of chemical species. Using the same set of samples as for the XRD analysis, FTIR spectra were obtained. Shown in Figure 7a are the FTIR spectra of the samples in the hydrogenation step. The starting imide $Li_2MgN_2H_2$ shows a broad N−H absorbance centered at about 3174 cm^{-1}. At $H = 0.33$ (point A), the typical absorbance of $LiNH_2$ at 3258 and 3312 cm^{-1} can be observed. This absorbance then persists from the sloping region through the hydrogenation plateau. At the end of hydrogenation of the PCI experiment, the spectrum shows mainly the absorbance of $Mg(NH_2)_2$ at 3272 and 3326 cm^{-1}. Nevertheless, the typical absorbance at 3258 and 3312 cm^{-1} for $LiNH_2$ can still be discerned, indicating that hydrogenation was not complete. This may be caused by insufficient hydrogen pressure and short delay time, which are limited by the

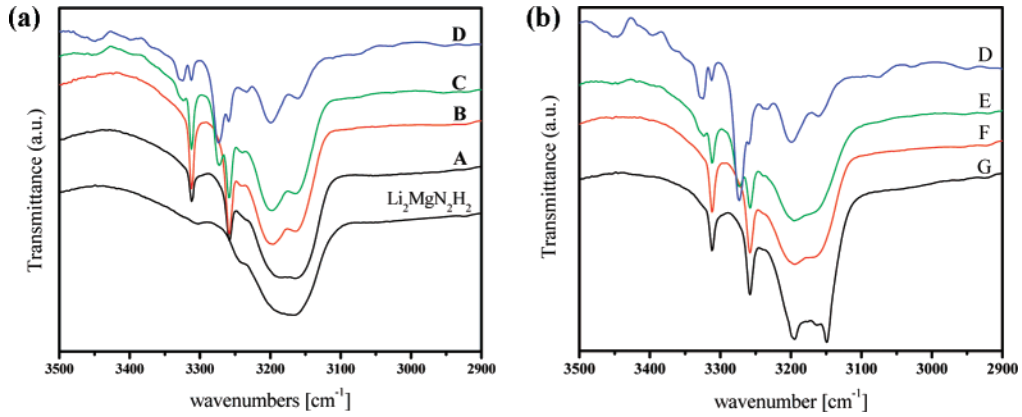

Figure 7. FTIR spectra of the samples at different PCI stages (capital letters denote the sampling points of the PCI experiments): (a) hydrogenation and (b) dehydrogenation.

instrument (upper pressure limit of 1000 psi). No $LiNH_2$ absorbance can be detected after prolonged hydrogenation (100 bar for 20 h) (not shown). In the dehydrogenation process (Figure 7b), the intensity of the $Mg(NH_2)_2$ absorbance at 3272 and 3326 cm^{-1} decreases. As can be seen in the dehydrogenation plateau region at $H = 2.60$, $Mg(NH_2)_2$ was substantially consumed, whereas the intensity of $LiNH_2$ absorbance increased. In the spectrum of $H = 1.5$, viz. the joint of the plateau with the slope, the absorbance of $Mg(NH_2)_2$ disappears completely. At $H = 0.86$, the absorbance of $LiNH_2$ disappears, leading to the formation of the starting ternary imide $Li_2MgN_2H_2$. As compared to the spectrum from the starting imide $Li_2MgN_2H_2$, however, the sample exhibits a relatively fine structure after the PCI experiment (one cycle of hydrogenation and dehydrogenation). This may be due to the improvement in the crystallinity of the sample during the hydrogen sorption process. Comparing the FTIR spectrum of the imide $Li_2Mg_2(NH)_3$ (Figure 3) in the prior section with that of the PCI sample at $H = 1.35$ (point F), it can be seen that the spectrum at point G exhibits absorbances of both $Li_2Mg_2(NH)_3$ and $LiNH_2$.

Chemical Reactions in Hydrogen Absorption/Desorption. Combining the FTIR and XRD results of the samples with different hydrogen contents, detailed chemical reactions involved in the hydrogenation/dehydrogenation processes were proposed. In the hydrogenation step, $Li_2MgN_2H_2$ was first converted to $Li_2Mg_2(NH)_3$ upon absorbing hydrogen. $Li_2Mg_2(NH)_3$ along with $LiNH_2$ and LiH then reacts with hydrogen to form $Mg(NH_2)_2$ and LiH. In the reverse dehydrogenation step, the amide and hydride take the same reaction route as in the hydrogenation and go back to $Li_2MgN_2H_2$. It is obvious that $Li_2Mg_2(NH)_3$ and $LiNH_2$ play the role of intermediates in the cycle of hydrogen absorption and desorption. The chemical events occurring in the process are suggested with the following reaction equations: in the slope region

$$2Li_2MgN_2H_2 + H_2 \leftrightarrow LiH + LiNH_2 + Li_2Mg_2(NH)_3 \quad (2)$$

and in the plateau region

$$LiNH_2 + Li_2Mg_2(NH)_3 + 3H_2 \leftrightarrow 3LiH + 2Mg(NH_2)_2 \quad (3)$$

Luo and Sickafoose reported a ternary imide with the composition of $Li_2MgN_2H_{3.2}$ as an intermediate in the hydrogen absorption/desorption process.[11] The authors proposed the following reaction for the slope region:

$$Li_2MgN_2H_2 + 0.6H_2 \leftrightarrow Li_2MgN_2H_{3.2} \quad (4)$$

The composition of the intermediate was obtained based on the inflection in the PCI curve. Recently, Aoki et al. reported two intermediates, $Li_4Mg_3(NH_2)_2(NH)_4$ and $Li_{4+x}Mg_3(NH_2)_{2-x}(NH)_{4+x}$, of orthorhombic structure in the Li−Mg−N−H system.[15] On the basis of the similarity of their XRD patterns to the peak positions of $Li_2MgN_2H_2$ in this study after the absorption/desorption cycle, the presence of the orthorhombic structure is clearly recognizable.

In contrast to the following ammonia-mediated mechanism:[16]

$$Mg(NH_2)_2 \leftrightarrow MgNH + NH_3 \quad (5)$$

$$LiH + NH_3 \leftrightarrow LiNH_2 + H_2 \quad (6)$$

it has been found in a recent paper by Chen et al. that reaction 5 of NH_3 generation from $Mg(NH_2)_2$ has a much higher apparent activation energy (130 kJ/mol) than that of the reaction of $Mg(NH_2)_2$ and 2LiH (88 kJ/mol); thus, thermal decomposition of $Mg(NH_2)_2$ is unlikely to be an elementary step in the chemical reaction of $Mg(NH_2)_2$ and 2LiH.[17] Moreover, exchange reactions between $H^{\delta+}$ in $Mg(NH_2)_2$ and $H^{\delta-}$ in LiH were detected by isotopic investigations, signaling a solid-state coordinated interaction between the amide and the hydride.

The observation of a solid ternary imide as an intermediate in this work and by other authors, albeit with some diversity in chemical composition, demonstrates that the chemical process of hydrogen absorption/desorption occurs among five solid-state components of $Mg(NH_2)_2$, LiH, $LiNH_2$, $Li_2MgN_2H_2$, and $Li_2Mg_2(NH)_3$ and one gaseous component H_2, which is supportive of the coordination mechanism.

Luo and Sickafoose made a phase analysis based on PCI results using the Gibbs phase rule for the elucidation of the chemistry occurring in the hydrogen absorption/desorption.[11] According to our results, it can be seen that there are five components in both eqs 2 and 3. For the plateau, the number of phases is five (i.e., $P = 5$), and the number of components is five minus one reaction equation (i.e., $C = 5 - 1 = 4$), and we obtain the number of degrees of freedom F by applying the Gibbs phase rule

$$F = C - P + 2 = 4 - 5 + 2 = 1 \quad (7)$$

which fits the relationship of phase and component for the plateau region. However, a problem arises when applying the Gibbs phase rule for the sloping part, as the numbers of phases and components seem to be the same as in the plateau part. While the chemical component $LiNH_2$ could clearly be detected

by FTIR, its existence as a phase cannot be unambiguously verified by XRD, due to its structural similarity to $Li_2MgN_2H_2$.[12] However, cancellation of $LiNH_2$ does not alter the fact that there may be the same numbers of phases and components in the plateau and sloping stages. Since the Gibbs phase rule is generally applicable in all systems, the number of phases has to be corrected by minus one for the sloping part.

This inconsistency of experimental observation with theoretical analysis may be caused by two factors. One is the amorphism and polymorphism of the reactant crystals resulting from the mechanical ball milling, which possibly prevents the observation of some phases. The other factor involved is the possible formation of eutectic phases or melts or cocrystals at the interface by local heating during the mechanochemical ball milling. In the inter-solid reactions, reactions can take place either on the crystallite surface or else require molecular diffusion through the lattice; in the latter case, the reactions are often accompanied by the formation of eutectics.[18] The formation of eutectic phases among the chemical species can lead to reduction in the number of phases. Mass transport could be facilitated if the reacting components existed in solid solutions. We assume that some sort of solid solutions might have resulted during hydrogen absorption/desorption, which would result in the reduction of the number of phases. More experiments have to be designed and conducted for the clarification of phase and crystal structure.

Conclusion

The chemical species at different stages of the hydrogen absorption/desorption process of the Li−Mg−N system were identified, revealing the same chemical species in the hydrogen absorption and desorption steps. A ternary imide with the composition of $Li_2Mg_2(NH)_3$ along with $LiNH_2$ were found to be the intermediates in the hydrogen sorption process. The chemical reactions for the sloping region and the plateau of the PCI curve were suggested. Following phase analysis, it is assumed that a solid solution might be formed during the mechanochemical treatments.

Acknowledgment. The authors acknowledge financial support from General Motors (U.S.) and the Agency for Science, Technology and Research (A*Star) (Singapore).

References and Notes

(1) Schlapbach, L.; Züttel, A. *Nature (London, U.K.)* **2001**, *414*, 353−358.
(2) Schüth, F.; Bogdanovic, B.; Felderhoff, M. *Chem. Commun.* **2004**, 2249−2258.
(3) Chen, P.; Xiong, Z.; Luo, J.; Lin, J.; Tan, K. L. *Nature (London, U.K.)* **2002**, *420*, 302−304.
(4) Chen, P.; Xiong, Z.; Luo, J.; Lin, J.; Tan, K. L. *J. Phys. Chem. B* **2003**, *107*, 10967−10970.
(5) Luo, W. *J. Alloys Compd.* **2004**, *381*, 284−287.
(6) Xiong, Z. T.; Wu, G. T.; Hu, J. J.; Chen, P. *Adv. Mater.* **2004**, *16*, 1522−1525.
(7) Leng, H. Y.; Ichikawa, T.; Hino, S.; Hanada, N.; Isobe, S.; Fujii, H. *J. Phys. Chem. B* **2004**, *108*, 8763−8765.
(8) Xiong, Z. T.; Hu, J. J.; Wu, G. T.; Chen, P.; Luo, W. F.; Gross, K.; Wang, J. *J. Alloys Compd.* **2005**, *398*, 235−239.
(9) Juza, R.; Eberius, E. *Naturwissenschaften* **1962**, *49*, 104.
(10) Xiong, Z. T.; Hu, J. J.; Wu, G. T.; Chen, P.; Luo, W. F.; Wang, J. *J. Alloys Compd.* **2006**, *417*, 190−194.
(11) Luo, W.; Sickafoose, S. *J. Alloys Compd.* **2006**, *407*, 274−281
(12) Rijssenbeek, J. et al. *J. Alloys Compd.* **2007**, [online early access] doi:10.1016/j.jallcom.2006.12.008.
(13) Janot, R.; Eymery, J.-B.; Tarascon, J.-M. *J. Power Sources* **2007**, *164*, 496−502.
(14) Aoki, M.; Noritake, T.; Nakamori, Y.; Towata, S.; Orimo, S. *J. Alloys Compd.* **2007**, *446*−*447*, 328−331.
(15) Aoki, M.; Noritake, T.; Kitahara, G.; Nakamori, Y.; Towata, S.; Orimo, S. *J. Alloys Compd.* **2007**, *428*, 307−311
(16) Leng, H.; Ichikawa, T.; Hino, S.; Nakagawa, T.; Fujii, H. *J. Phys. Chem. B* **2005**, *109*, 10744−10748.
(17) Chen, P.; Xiong, Z. T.; Yang, L. F.; Wu, G. T.; Luo, W. F. *J. Phys. Chem. B* **2006**, *110*, 14221−14225.
(18) Toda, F. *Topics in Current Chemistry: Organic Solid State Reactions*; Springer: Berlin, 2005; Vol. 254.